Heteroatom Chemistry
Volume 9, Number 1, 1998

# Triphospholes as **2e** and **4e** Donors: Synthesis and Structural Characterization of the 1,2,4-Triphosphole Complexes $\eta^1$-*trans*-$[PtCl_2(PEt_3)(P_3C_2Bu^t_2CH(SiMe_3)_2]$ and $\eta^1$-$\eta^1$-*trans*-$[PtCl_2(PEt_3)_2\}_2(\mu\text{-}P_3C_2Bu^t_2CH(SiMe_3)_2]$

Vinicius Caliman, Peter B. Hitchcock, and J. F. Nixon*

*School of Chemistry, Physics and Environmental Science, University of Sussex, Falmer, Brighton BN1 9QJ, U.K.*

*Received 31 March 1997*

## ABSTRACT

*The first examples of $\eta^1$-complexes of 1,2,4-triphospholes are reported in which the ring acts as a* **2e** *and a* **4e** *donor.* © 1998 John Wiley & Sons, Inc. Heteroatom Chem **9**:1–8, 1998

## INTRODUCTION

We recently reported [1] the first example of a 1,2,4-triphosphole (**1**) (Equation 1) formed by alkylation of the aromatic $P_3C_2Bu^t_2$ ring anion.

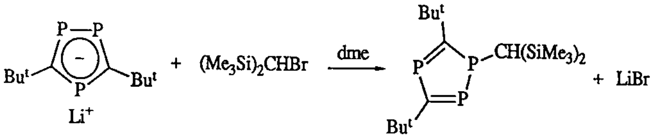

(1)

Compound (**1**) exhibits a variety of ligating behavior; for example, it behaves as a **6e** donor in $[Fe_2(CO)_6[P_3C_2Bu^t_2\,CH(SiMe_3)_2]]$ where the ring is severely buckled [1]. Of special interest is the greatly enhanced aromatic behavior of the 1,2,4-triphosphole ring system (**1**) compared with phospholes themselves, and in its complexes with both $[M(CO)_3]$ fragments (M = Cr, Mo, W) and with [Ru(0) (cyclooctadiene)], it is also a **6e** donor, but now the ring is essentially planar [2,3]. In a preliminary report [1], we also described the ligating behavior of the 1,2,4-triphosphole as a **2e** donor in *trans*-$[PtCl_2(PEt_3)[P_3C_2Bu^t_2CH(SiMe_3)_2]]$ (**2**). Here we report in full on this complex and its further unexpected reaction to ligate a second platinum(II) fragment, in which the ring is acting as a **4e** donor.

## DISCUSSION

### *Synthesis of trans-$[PtCl_2(PEt_3)\{P_3C_2Bu^t_2CH(SiMe_3)_2\}]$* (**2**)

The 1,2,4-triphosphole (**1**) reacts with a half equivalent of $[PtCl_2(PEt_3)]_2$ in petroleum ether 60–80°C to give the monosubstituted product $[PtCl_2(PEt_3)[P_3C_2Bu^t_2CH(SiMe_3)_2]]$ (**2**), as shown in Equation 2:

---

Dedicated to Prof. William E. McEwen on the occasion of his seventy-fifth birthday.

*To whom correspondence should be addressed.

CCC 1042-7163/98/010001-08

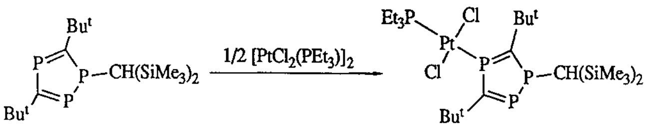

(2)

The reaction proceeds readily at room temperature and is complete within 4 hours. Only a slight excess of the ligand is required, otherwise a di-platinum(II) product can also be formed (vide infra).

$^{31}P\{^{1}H\}$ NMR spectroscopy was employed to monitor the course of the reaction, and the mode of attachment of the 1,2,4-triphosphole ring to platinum in (**2**) was established as unexpectedly being via the *sp*$^2$-hybridized phosphorus lying between the two carbon atoms. Complex (**2**) is the first example of an $\eta^1$-ligated triphosphole metal complex.

The 101.3 MHz $^{31}P\{^{1}H\}$ NMR spectrum of (**2**) is shown in Figure 1. It features the pattern typical of an [AMNX] spin system with the presence of satellite subspectra due to $^{195}$Pt(I = 1/2, 33.8%). The [AMN] spin system for the ring framework is quite distinct ($\delta$ P(A) 112.9, $\delta$ P(M) 201.5, and $\delta$ P(N) 194.9 ppm) from that of the *trans*-PEt$_3$ resonance ($\delta$ P(X) 12.0 ppm) that, as expected, appears at a higher field. The chemical shifts of P(M) and P(N) are typical for an *sp*$^2$-hybridized phosphorus atom, while P(A) corresponds to an *sp*$^3$ phosphorus atom. The splitting patterns observed are as expected for the proposed static structure, with a large one-bond coupling between the phosphorus atoms P(A) and P(M) ($^1J_{P(A)P(M)}$ 492.2 Hz). The observation of the large two-bond coupling between P(N) and P(X) ($^2J_{P(N)P(X)}$ 503.1 Hz) establishes that they are in mutually *trans*-positions. Several other small couplings, over two and three bonds, can be seen for all phosphorus resonances. P(X), P(N), and P(A) each show Pt satellites [$^1J_{P(X)Pt}$ 2913.6, $^1J_{P(N)Pt}$ 2368.5, and $^3J_{P(A)Pt}$ 110.8 Hz].

The $^{195}Pt\{^{1}H\}$ NMR spectrum of (**2**) confirms the above structural proposals exhibiting a single Pt resonance ($\delta$ Pt-3676 ppm), which lies in the range observed for *trans*-[PtCl$_2$(PR$_3$)$_2$] complexes (R = alkyl, aryl). This resonance is split into a doublet of doublets of doublets arising from couplings to the three types of phosphorus atoms.

Compound (**2**) is also readily identified from the analysis of its mass spectrum that exhibits the molecular ion showing the expected isotopic distribution. A computer simulation was carried out for the parent ion complex and exactly matches the experimental results.

### *Crystal and Molecular Structure of [PtCl$_2$(PEt$_3$){P$_3$C$_2$Bu$^t_2$CH(SiMe$_3$)$_2$}] (2)*

A single-crystal X-ray diffraction study was performed on *trans*-[PtCl$_2$(PEt$_3$)[P$_3$C$_2$Bu$^t_2$CH(SiMe$_3$)$_2$]]

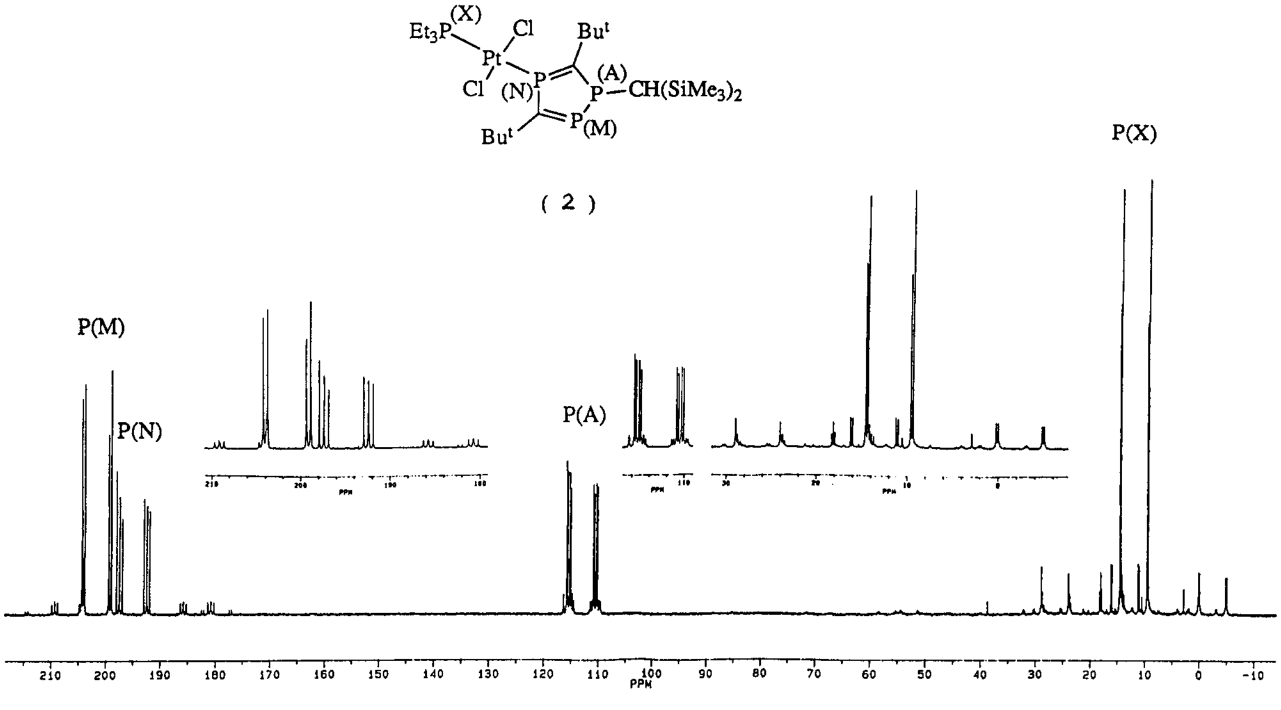

**FIGURE 1** $^{31}P\ \{^{1}H\}$ NMR spectrum of *trans*-[PtCl$_2$(PEt$_3$){P$_3$C$_2$Bu$^t_2$CH(SiMe$_3$)$_2$}] (**2**) in CDCl$_3$ at 25°C.

(**2**), and the molecular structure shown in Figure 2 was established. Several important features of interest are evident. Comparison of the bond lengths within the ring framework with the same bonds in the free ligand shows that the P(2)–C(2) distances are similar [1.718(4) Å in (**1**), 1.758(13) Å in (**2**)]; likewise, the P(3)–C(2) distances are similar [1.763(4) Å in (**1**) and 1.737(12) Å in (**2**)]. The planarity of P(1) has increased slightly, as shown by the sum of its bond angles, 342.3° in (**1**) versus 345.6° in (**2**), suggesting that the electronic delocalization is greater in the $\eta^1$-complexed ligand.

The unsaturated P(3) atom that is coordinated to the Pt center, is as expected planar, as shown by the sum of its bond angles (359.9°). The coordination sphere of the platinum atom is approximately square planar, and the angles between two groups *trans* to each other are typical. The Pt–Cl distances [2.315(3) and 2.305(3) Å] and the Pt–P distances [Pt–P(3) = 2.326(3) and Pt–P(4) = 2.283(3) Å] are also typical of those observed in related platinum(II) complexes [4–8]. However, the metal-ring Pt–P(3) bond distance is significantly longer than the Pt–P(4) bond distance of the $PEt_3$ ligand, reflecting that this is the weaker Pt–P bond.

### *Synthesis of trans-[{PtCl$_2$(PEt$_3$)}$_2${μ-P$_3$C$_2$Bu$^t_2$CH(SiMe$_3$)$_2$}] (3)*

Treatment of (**2**) with a further half equivalent of $[PtCl_2(PEt_3)]_2$ affords the dinuclear platinum(II) complex *trans*-[{$PtCl_2(PEt_3)$}$_2${$\mu$-$P_3C_2Bu^t_2CH(SiMe_3)_2$}] (**3**). The second Pt(II) coordination in (**3**) unexpectedly occurs via the $sp^3$-hybridized phosphorus (Equation 3), which is the most sterically hindered.

The $^{31}P\{^1H\}$ NMR spectrum of (**3**) shown in Figure 3 consists of an [AMNXY] spin system with satellite subspectra due to the two Pt atoms ($^{195}Pt$, I = 1/2, 33.8%). The evidence that the second Pt fragment is bonded to the $sp^3$-phosphorus atom in a *trans*-position is shown by the appearance of the resonance of P(Y) at 13.7 ppm with large P–P coupling constants [$^2J_{P(Y)P(A)}$ 403.9 Hz] and Pt satellites

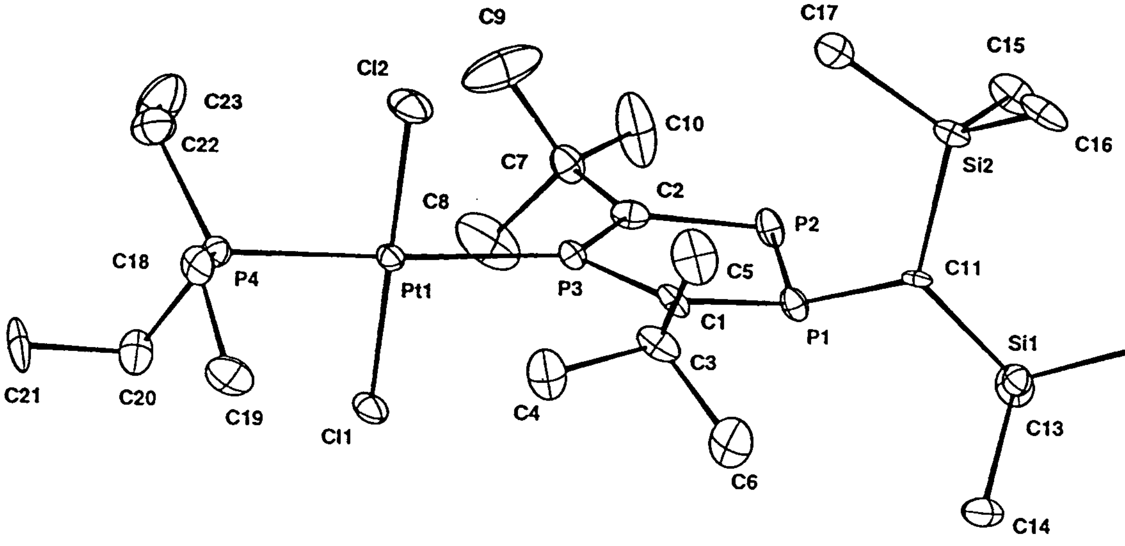

**P(1)-P(2) = 2.086(4), P(1)-C(1) = 1.738(11), P(3)-C(1) = 1.721(11),P(3)-C(2) = 1.737(12), P(2)-C(2) =1.758(13), P(1)-C(11) = 1.820(11), P(3)-Pt = 2.326(3), P(4)-Pt = 2.283(3), Cl(1)-Pt = 2.305(3), Cl(2)-Pt = 2.315(3), P(2)-P(1)-C(1) = 107.4(4), P(2)-P(1)-C(11) = 115.6(4), C(1)-P(1)-C(11) = 122.6(5), P(1)-P(2)-C(2) = 95.7(4), P(2)-C(2)-P(3) = 118.1(7), P(1)-C(1)-P(3) = 110.4(6), C(1)-P(3)-C(2) = 107.7(6), Pt-P(3)-C(1) = 126.0(4), Pt-P(3)-C(2) = 126.2(4), P(3)-Pt-P(4) = 176.33(12), Cl(1)-Pt-Cl(2) = 179.42(14).**

**FIGURE 2** Molecular structure of *trans*-[$PtCl_2(PEt_3)$]{$P_3C_2Bu^t_2CH(SiMe_3)_2$}] (**2**) together with the atomic numbering scheme and some selected bond lengths (Å) and bond angles (°).

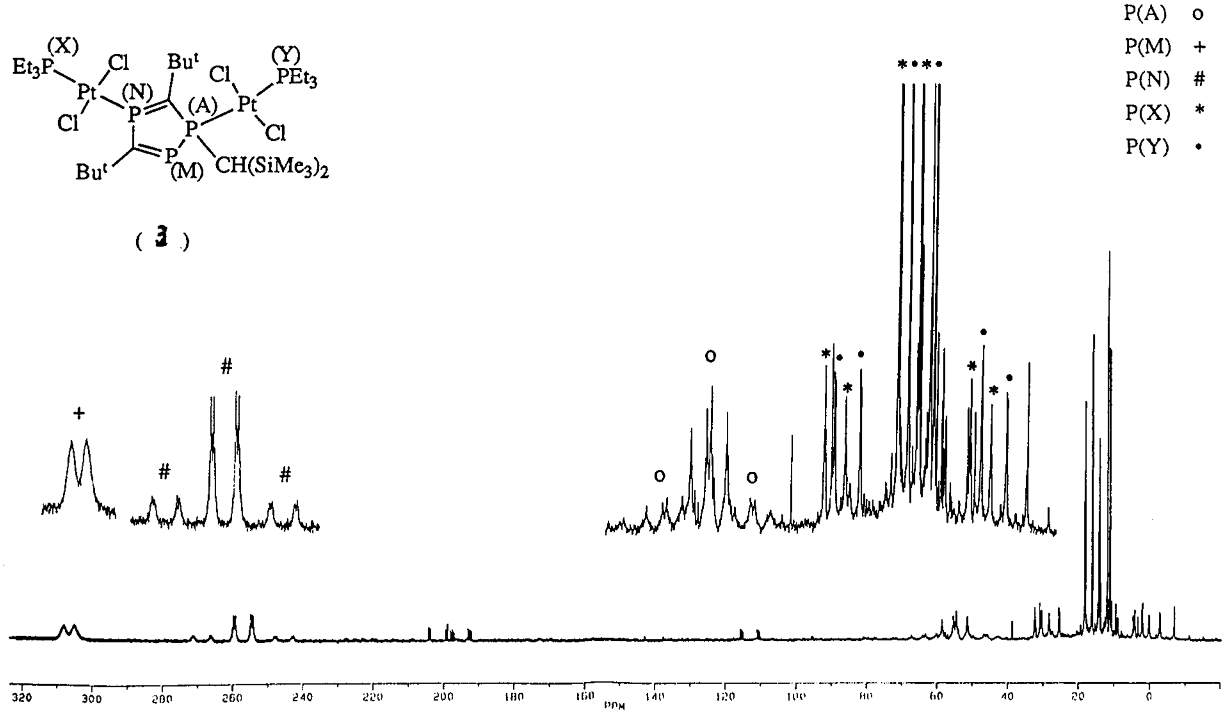

**FIGURE 3** $^{31}P$ $\{^1H\}$ NMR spectrum of *trans*-$[\{PtCl_2(PEt_3)\}_2\{\mu\text{-}P_3C_2Bu^t_2CH(SiMe_3)_2\}]$ (**3**) in $CDCl_3$ at 25°C.

[$^1J_{P(Y)Pt(B)}$ 2871.4 Hz], and this was subsequently confirmed by a single-crystal X-ray diffraction study (vide infra).

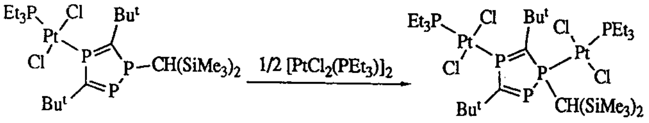

(3)

The $^{31}P\{^1H\}$ NMR spectra of (2) and (3) are quite similar, and a comparison of their chemical shift and coupling constant data is summarized in Table 1.

An important feature arising from the chemical shift data is that the resonance of P(A) has moved significantly to high field in (3) due to the coordination of a Pt metal fragment, increasing the $sp^3$ character in this phosphorus. The shifts of P(M) and P(N) also have moved significantly; however, their low-field chemical shifts shown in (3) indicate that the $sp^2$ hybridization in these two phosphorus is retained.

### *Crystal and Molecular Structure of trans-$[\{PtCl_2(PEt_3)\}_2\{\mu\text{-}P_3C_2Bu^t_2CH(SiMe_3)_2\}]$ (3)*

The proposed molecular structure for complex (3) deduced from the solution $^{31}P\{^1H\}$ NMR spectroscopic data was confirmed in the solid state. A single-

**TABLE 1** Summary of the Chemical Shift and Coupling Constant Data from the $^{31}P$ $[^1H]$ NMR Spectrum of *trans*-$[PtCl_2(PEt_3)\{P_3C_2Bu^t_2CH(SiMe_3)_2\}]$ (**2**) and *trans*-$[\{PtCl_2(PEt_3)\}_2\{\mu\text{-}P_3C_2Bu^t_2CH(SiMe_3)_2\}]$ (**3**)†

| 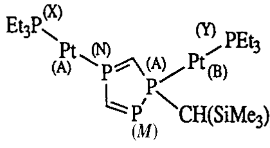 |  | (2) | (3) | $\Delta\delta$ |
|---|---|---|---|---|
| Chemical shifts (ppm)[a] | P(A) | 112.9 | 54.8 | −58.1 |
|  | P(M) | 201.5 | 306.4 | 104.9 |
|  | P(N) | 194.9 | 257.0 | 62.1 |
|  | P(X) | 12.0 | 16.2 | 4.4 |
|  | P(Y) |  | 13.7 |  |
| Coupling constants (Hz)[a] | $^1J_{P(A)P(M)}$ | 492.2 | 313.8 |  |
|  | $^2J_{P(N)P(X)}$ | 503.1 | 504.3 |  |
|  | $^2J_{P(A)P(Y)}$ |  | 403.9 |  |
|  | $^2J_{P(M)P(N)}$ | 49.0 | 61.4 |  |
|  | $^1J_{Pt(A)P(N)}$ | 2368.5 | 2360.0 |  |
|  | $^1J_{Pt(A)P(X)}$ | 2913.6 | 2851.3 |  |
|  | $^1J_{Pt(B)P(A)}$ |  | 1759.5 |  |
|  | $^1J_{Pt(B)P(Y)}$ |  | 2871.4 |  |

[a] As indicated at the top of the table.

†$Bu^+$ groups omitted for clarity.

crystal X-ray diffraction study shows the molecular structure presented in Figure 4.

The symmetry around the two Pt atoms in (**3**) is very close to the ideal square planar geometry, with the four Pt–Cl distances lying in the range 2.297–2.303 Å, which is typical for platinum(II) complexes. Both Pt(1)–P(4) and Pt(2)–P(5) bond distances [2.281(4) and 2.288(3) Å, respectively] are as expected. The metal-ring bond distance Pt(1)–P(1) [2.373(3) Å], however, is longer than the other metal-ring bond distance Pt(2)–P(3) [2.310(3) Å], reflecting the effects of a weaker Pt–P bond. The bond lengths within the ring framework are summarized in Table 2, together with the corresponding bond lengths for *trans*-$[\{PtCl_2(PEt_3)\{P_3C_2Bu^t_2CH(SiMe_3)_2\}]$ (**2**) and $P_3C_2Bu^t_2CH(SiMe_3)_2$ (**1**) itself.

Interestingly, unlike (**2**) and (**1**), the molecular structure of (**3**) is the only one that shows the bond lengths expected for the presence of a diene fragment. The two P = C double bonds P(2)–C(2) and P(3)–C(1) [1.665(11) Å and 1.667(10) Å, respectively] are the shortest of the three compounds and lie in the same range as those previously reported (1.64–1.69 Å) [9–15]. Compound (**3**) also shows the longest P–C [P(3)–C(2) = 1.797(10) Å and P(1)–C(1) = 1.832(9) Å] distances, which are comparable with those values expected for P–C (1.78–1.92 Å); likewise, the [P(1)–P(2)] = 2.172(4) Å distance is that

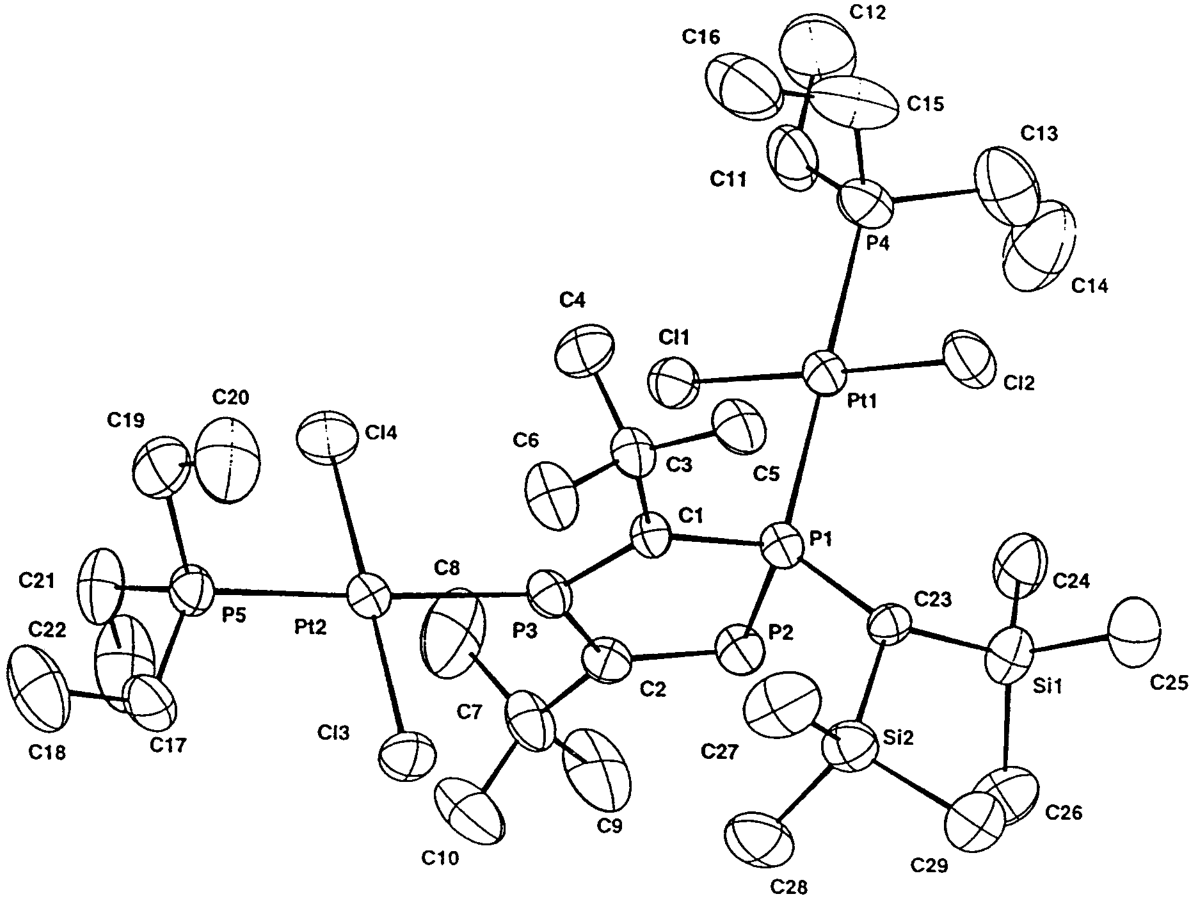

P(1)-P(2) = 2.172(4), P(1)-C(1) = 1.832(9), P(3)-C(1) = 1.667(10),P(3)-C(2) = 1.797(10), P(2)-C(2) =1.665(11), P(1)-C(23) = 1.854(9), P(1)-Pt(1) = 2.373(3), P(4)-Pt(1) = 2.281(4), P(3)-Pt(2) = 2.310(3), P(5)-Pt(2) = 2.288(3), Cl(1)-Pt(1) = 2.303(3), Cl(2)-Pt(1) = 2.297(3), Cl(3)-Pt(2) = 2.299(3), Cl(4)-Pt(2) = 2.303(3), C(1)-P(1)-P(2) = 102.1(3), C(1)-P(1)-C(23) = 115.2(4), P(2)-P(1)-C(23) = 103.8(3), P(1)-Pt(1)-P(4) = 178.18(12), Cl(1)-Pt(1)-Cl(2) = 178.22(12), P(3)-Pt(2)-P(5) = 177.61(11), Cl(3)-Pt(2)-Cl(4) = 179.26(13).

**FIGURE 4** Molecular structure of *trans*-$[\{PtCl_2(PEt_3)\}_2\{\mu\text{-}P_3C_2Bu^t_2CH(SiMe_3)_2\}]$ (**3**) together with the atomic numbering scheme and some selected bond lengths (Å) and bond angles (°).

**TABLE 2** Selected Bond Lengths (Å) for Compounds (*4*)–(*3*)

| 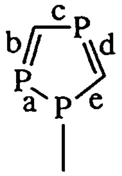 | *(1)* | *(2)* | *(3)* |
|---|---|---|---|
| P(1)–P(2)[a] | 2.098(1) | 2.086(4) | 2.172(4) |
| P(2)–C(2)[b] | 1.718(4) | 1.758(13) | 1.665(11) |
| P(3)–C(2)[c] | 1.763(4) | 1.737(12) | 1.797(10) |
| P(3)–C(1)[d] | 1.720(3) | 1.721(11) | 1.667(10) |
| P(1)–C(1)[e] | 1.734(4) | 1.738(11) | 1.832(9) |

[a,b,c,d,e] As indicated at the top of the table.

expected for a single bond [typically, 2.171–2.266 Å] [15,16]. The ring [P(1)P(2)C(1)P(3)C(2)] is planar in (**3**), while in (**1**) and (**2**) only the atoms from the diene system [P(2)C(1)P(3)C(2)] lie in the same plane. The P(1) to plane distance is 0.232 Å for (**1**) and 0.170 Å for (**2**), and the bond angles around this phosphorus, excluding Pt, are typical for a $sp^3$-hybridized atom ($\Sigma_{\text{angles}} = 321.1°$).

## *EXPERIMENTAL*

Standard procedures for the manipulation of air-sensitive materials were employed. All manipulations were carried out at ambient temperature under an atmosphere of dry nitrogen gas (or argon) using standard Schlenk, syringe, and high vacuum-line techniques, with glassware that had been flame-dried in vacuo prior to use.

Solvents (tetrahydrofuran, 1,2-dimethoxyethane, diethyl ether, and petroleum ether) were dried, freshly distilled under a blanket of dinitrogen, and degassed prior to use. A sodium-potassium alloy was used as a drying agent. Mass spectra were recorded at the University of Sussex by Dr. A. Abdul-Sada and Mr. A. M. Greenway using a Fison-VG Autospec or a Kratos MS-80 RF mass spectrometer. Solution NMR spectra were recorded on Brüker ACP-250, WM-360, or AMX-500 instruments at ambient probe temperature.

### *Starting Materials*

The following compounds were synthesized according to literature methods: $P(SiMe_3)_3$ was prepared from sodium, white phosphorus, and $Me_3SiCl$ [17]; $(Me_3Si)P{=}C(OSiMe_3)(Bu^t)$ from $P(SiMe_3)_3$, and $Bu^tCOCl$ [18] $[Li(P_3C_2Bu^t_2)]$ was prepared as follows using a method developed in this laboratory [19] based upon an initial communication by Becker *et al.* [20]. A hexane solution of $LiBu^n$ (1.6 M, 10 mL, 16 mmol) was added to a DME solution of $P(SiMe_3)_3$ (2.0 g, 8 mmol in 10 mL) at 0°C. The resulting yellow solution was stirred for 3 hours and allowed to warm slowly to ambient temperature. Stirring was continued for a further 20 hours to give an off-white cloudy mixture, and $(Me_3Si)P{=}C(OSiMe_3)(Bu^t)$(4.5 g, 17 mmol) was then added and the mixture stirred for a further 24 hours. During this time, an orange-red color developed that gradually darkened until it was almost black. The volatile components were removed in vacuo and the oily residue washed with hexane (2 × 25 mL). The resulting oil was characterized by $^{31}P\{^1H\}$ NMR spectroscopy and used without further purification as a stock solution in DME.

### *Synthesis of $P_3C_2Bu^t_2CH(SiMe_3)_2$ (1)*

$Li(P_3C_2Bu^t_2)$ (2.31 mmol) in DME (10 mL) was added slowly to a solution of $HCBr(SiMe_3)_2$ (0.6 mL, 2.31 mmol) in DME (15 mL) at −30°C, and the resulting mixture was stirred for 20 hours. The LiBr formed during the reaction was filtered off and the solvent evaporated in vacuo. The residue was purified by column chromatography (kiesel gel/p.e. 60–80°C) to give an orange oil (400 mg, 44%) that was characterized as 1-bis-trimethylsilylmethyl-1,2,4-triphospha-3,5-*tert*-butyl-cyclopentadiene. Recrystallization from p.e. 60–80°C at room temperature afforded orange crystals (m.p. = 79–80°C). Found: C = 51.5, H = 9.4; $C_{17}H_{37}P_3Si_2$ requires C = 52.3, H = 9.6%.

### *$^{31}P\{^1H\}$ NMR Data (101.3 MHz, Chloroform-$d_1$, 25°C)*

$\delta$ 244.4 ppm [dd, P(Y), $^2J_{P(Y)P(A)}$ 8.0 Hz, $^2J_{P(Y)P(X)}$ 44.1 Hz]; $\delta$ 180.0 ppm [dd, P(X), $^1J_{P(X)P(A)}$ 509.5 Hz, $^2J_{P(X)P(Y)}$ 44.1 Hz]; $\delta$ 112.0 ppm [dd, P(A), $^1J_{P(A)P(X)}$ 509.5 Hz, $^2J_{P(A)P(Y)}$ 8.0 Hz].

### *$^{29}Si\{^1H\}$ NMR Data (49.7 MHz, Chloroform-$d_1$, 25°C)*

$\delta$ 4.12 ppm [ddd, Si, $^2J_{SiP(A)}$ 6.56 Hz, $^3J_{SiP(X)}$ 2.10 Hz, $^4J_{SiP(Y)}$ 0.71 Hz].

### *$^{13}C\{^1H\}$ NMR Data (62.9 MHz, Chloroform-$d_1$, 25°C)*

$\delta$ 204.7 [ddd, *C*C $(CH_3)_3$, $^1J_{CP}$ 72.85 Hz, $^1J_{CP}$ 66.94 Hz, $^2J_{CP}$ 21.66 Hz]; $\delta$ 188.8 [ddd, *C*C $(CH_3)_3$, $^1J_{CP}$ 69.90 Hz, $^1J_{CP}$ 39.38 Hz, $^2J_{CP}$ 8.86 Hz]; $\delta$ 41.6 [ddd, *C*C $(CH_3)_3$, $^2J_{CP}$ 21.66 Hz, $^2J_{CP}$ 19.69 Hz, $^3J_{CP}$ 6.89 Hz]; $\delta$ 40.2 [d, C*C* $(CH_3)_3$, $^2J_{CP}$ 17.72 Hz]; $\delta$ 35.7 [m, $C(CH_3)_3$; $\delta$ 20.9

ppm (dd, *C*H, $^1J_{CP}$ 40.36 Hz, $^2J_{CP}$ 4.92 Hz]; $\delta$ 0.7 (s, $[Si(CH_3)_3]_2$, $^1J_{CSi}$ 52.9 Hz).

### *$^1$H NMR Data (250.2 MHz, Chloroform-$d_1$, 25°C)*

$\delta$ 0.15 [s, 18H, $[Si(CH_3)_3]_2$]; $\delta$ 1.57 [d, 9H, $C(CH_3)_3$, $^4J_{HP}$ 1.23 Hz]; $\delta$ 1.59 [d, 9H, $C(CH_3)_3$, $^4J_{HP}$ 1.73 Hz]; $\delta$ 2.06 (dd, 1H, CH, $^2J_{HP}$ 15.0 Hz, $^3J_{HP}$ 12.1 Hz).

### *Mass Spectrum (EI)*

m/z: 390 $[(P_3C_2Bu^t_2)CH(SiMe_3)_2]^+$ (16%), 317 $[(P_3C_2Bu^t_2)CH(SiMe_3)]^+$, 231 $[P_3C_2Bu^t_2]^+$, 169 $[P_3C_2Bu^t_2]^+$, 73 $[SiMe_3]^+$.

### *Synthesis of trans-$[PtCl_2(PEt_3)\{P_3C_2Bu^t_2CH(SiMe_3)_2\}]$* (**2**)

$[PtCl_2(PEt_3)]_2$ (290 mg, 0.38 mmol) was added as a solid to a solution of $P_3C_2Bu^t_2CH(SiMe_3)_2$ (320 mg, 0.82 mmol) in p.e. 60–80°C (10 mL) and stirred for 4 hours. The yellow solid was filtered off and washed with p.e. 60–80°C (5 mL) to give *trans*-$[PtCl_2(PEt_3)\{P_3C_2Bu^t_2CH(SiMe_3)_2\}]$ (550 mg, 92%). Recrystallization from THF/p.e. 30–40°C gave yellow crystals (m.p. = 155°C). The compound was characterized on the basis of $^{31}$P and $^1$H NMR spectroscopy, mass spectroscopy, and elemental analysis. Found: C = 34.2, H = 6.5; $C_{23}H_{52}Cl_2P_4PtSi_2$ requires C = 35.7, H = 6.8%). The structure was confirmed by a single-crystal X-ray diffraction study.

### *$^{195}$Pt{$^1$H} NMR Data (53.8 MHz, Chloroform-$d_1$, 25°C)*

$\delta$-3676 [ddd, Pt, $^1J_{PtP(X)}$ 2913.6 Hz, $^1J_{PtP(N)}$ 2368.5 Hz, $^3J_{PtP(A)}$ 110.8 Hz].

### *$^{31}$P{$^1$H} NMR Data (53.8 MHz, Chloroform-$d_1$, 25°C)*

$\delta$ 201.5 [dd, P(M), $^1J_{P(M)P(A)}$ 492.2 Hz, $^2J_{P(M)P(N)}$ 49.0 Hz]; $\delta$ 194.9 [ddd, P(N), $^1J_{P(N)Pt}$ 2368.5 Hz, $^2J_{P(N)P(X)}$ 503.1 Hz, $^2J_{P(N)P(A)}$ 53.5 Hz, $^2J_{P(N)P(M)}$ 49.0 Hz]; $\delta$ 112.9 [ddd, P(A), $^3J_{P(A)Pt}$ 110.8 Hz, $^1J_{P(A)P(M)}$ 492.2 Hz, $^1J_{P(A)P(M)}$ 492.2 Hz, $^2J_{P(A)P(N)}$ 53.5 Hz, $^4J_{P(A)P(X)}$ 23.4 Hz]; $\delta$ 12.0 [dd, P(X), $^1J_{P(X)P(N)}$ 503.1 Hz, $^4J_{P(X)P(A)}$ 23.4 Hz].

### *$^1$H NMR Data (250.2 MHz, Chloroform-$d_1$, 25 °C)*

$\delta$ 0.09 (s, 18H, $[Si(CH_3)_3]_2$); $\delta$ 1.16 [dt, 9H, $(CH_2CH_3)_3$, $^3J_{HP}$ 17.02 Hz, $^3J_{HH}$ 7.52 Hz]; $\delta$ 1.79 [s, 9H, $C(CH_3)_3$]; $\delta$ 1.80 [s, 9H, $C(CH_3)_3$]; $\delta$ 1.86 [m, 6H, $(CH_2CH_3)_3$]; $\delta$ 2.12 (dd, 1H, *C*H, $^2J_{HP}$ 28.55 Hz, $^3J_{HP}$ 1.25 Hz).

### *Mass Spectrum (EI)*

m/z: 774 $[(PtCl_2(PEt_3)[P_3C_2Bu^t_2CH(SiMe_3)_2]]^+$, (19%), 390 $[P_3C_2Bu^t_2CH(SiMe_3)]^+$, 231 $[P_3C_2Bu^t_2]^+$, 73 $[SiMe_3]^+$.

### *Synthesis of trans-$[\{PtCl_2(PEt_3)\}_2\{\mu\text{-}P_3C_2Bu^t_2CH(SiMe_3)_2\}]$* (**3**)

A mixture of *trans*-$[PtCl_2(PEt_3)\{P_3C_2Bu^t_2CH(SiMe_3)_2\}]$ (460 mg, 0.60 mmol) and $[PtCl_2(PEt_3)]_2$ (230 mg, 0.30 mmol) was stirred in chloroform (5 mL) for 4 hours at room temperature. The solvent was pumped off and the yellow solid washed with p.e. 60–80°C (2 × 3 mL) and dried in vacuo to give *trans*-$[\{PtCl_2(PEt_3)\}_2\ \{\mu\text{-}P_3C_2Bu^t_2CH(SiMe_3)_2\}]$ (420 mg, 60% yield). Recrystallization from THF/p.e. 30–40°C gave single crystals (mp = 155°C) for the X-ray diffraction study.

*$^{31}$P{$^1$H} NMR Data (101.3 MHz, Chloroform-$d_1$, 25°C* $\delta$ 306.4 [dm, P(M), $^1J_{P(M)P(A)}$ 313.8 Hz, $^2J_{P(M)P(N)}$ 61.4 Hz]; $\delta$ 257.0 [dddd, P(N), $^1J_{P(N)Pt(A)}$ 2360.0 Hz, $^2J_{P(N)P(X)}$ 504.3 Hz, $^2J_{P(N)P(M)}$ 61.4 Hz, $^2J_{P(N)P(A)}$ 24.2 Hz, $^4J_{P(N)P(Y)}$ 20.0 Hz]; $\delta$ 54.8 [dddd, P(A), $^1J_{P(A)Pt(B)}$ 1759.5 Hz, $^1J_{P(A)P(M)}$ 313.8 Hz, $^2J_{P(A)P(Y)}$ 403.9 Hz, $^2J_{P(A)P(N)}$ 24.2 Hz, $^4J_{P(A)P(X)}$ 23.2 Hz]; $\delta$ 16.2 [dd, P(X), $^1J_{P(X)Pt(A)}$ 2851.3 Hz, $^2J_{P(X)P(N)}$ 504.3 Hz, $^4J_{P(X)P(A)}$ 23.2 Hz], $\delta$ 13.7 [ddd, P(Y), $^1J_{P(Y)Pt(B)}$ 2871.4 Hz, $^2J_{P(Y)P(A)}$ 403.9 Hz, $^3J_{P(Y)P(M)}$ 20.2 Hz, $^4J_{P(Y)P(N)}$ 20.0 Hz].

### *Crystallographic Data*

*For Compound (2).* $C_{23}H_{52}Cl_2PtP_4Si_2$, M = 774.7, orthorhombic, a = 11.712(3), b = 11.834(2), c = 25.073(5) Å; $V$ = 3475.1(13) Å$^3$, $Z$ = 4, $d_c$ = 1.48 Mg/m$^3$, space group $P2_12_12_1$ $\mu$ = 4.46 mm$^{-1}$, F(000) = 1560, X-ray wavelength 0.71073 Å.

Crystallographic measurements were carried out at 293(2) K using an Enraf-Nonius CAD4 diffractometer on a crystal of 0.30 × 0.30 × 0.30 mm dimensions. Data were collected in the $\theta$ range 2°–25° .3431 reflections were collected, and 3102 had I > 2$\sigma$(I). The structure was solved using direct methods and refined by full-matrix least squares. The final R indices I > 2$\sigma$(I) were $R_1$ = 0.043; $w$R2 = 0.111 (all data). All non-H atoms were anisotropic. H atoms were included in riding mode with $U_{iso}$(H) equal to 1.2 U eq (C) for CH or $CH_2$ groups, or 1.5 U eq (C) for methyl groups. Coordinates and temperature factors are deposited at the Cambridge Crystallographic Data Centre.

*For Compound (***3***).* $C_{29}H_{67}Cl_4Pt_2P_5Si_2$, M = 1158.8, monoclinic, a = 18.176(4), b = 13.889(9), c = 20.198(12) Å, $\beta$ = 115.27(3)°, $V$ = 4611(4) Å$^3$, $Z$

= 4, $d_c$ = 1.67 Mg/m$^3$, space group $P2_1/c$ (No. 14), $\mu$ = 6.54 mm$^{-1}$ F(000) = 2272.

Crystallographic measurements were carried out at 293(2) K using an Enraf–Nonius CAD4 diffractometer on a crystal of 0.50 × 0.30 × 0.10 mm dimensions. Data were collected in the $\theta$ range 2°–25° .8363 reflections were collected, and 5195 had $I > 2\sigma(I)$. The structure was solved using direct methods and refined by full-matrix least squares. The final R indices were $R_1 = 0.053$; $wR2 = 0.121$ (all data). All non-H atoms were anisotropic. H atoms were included as in structure (2) above. Coordinates and temperature factors are deposited at the Cambridge Crystallographic Data Centre. Both structures were refined on all $F^2$ using SXELXL-93.

## ACKNOWLEDGEMENTS

We thank the Brazilian Government for financial support for V.C. (via CNP*q*) and EPSRC for their general support for phospha-alkyne chemistry at Sussex.

## REFERENCES

[1] V. Caliman, P. B. Hitchcock, J. F. Nixon, *J. Chem. Soc. Chem. Commun.*, 1995, 1661.
[2] V. Caliman, P. B. Hitchcock, J. F. Nixon, L. Nyulaszi, N. Sakarya, *J. Chem. Soc. Chem. Commun.*, 1997, 1305.
[3] P. B. Hitchcock, J. F. Nixon, N. Sakarya, *J. Chem. Soc. Chem. Commun.*, 1996, 2751.
[4] P. B. Hitchcock, J. F. Nixon, G. J. D. Sillett, *New J. Chem., 13,* 1989, 353.
[5] R. Bartsch, D. Carmichael, P. B. Hitchcock, M. F. Meidine, J. F. Nixon, *J. Chem. Soc. Chem. Commun.*, 1988, 1615.
[6] G. G. Messmer, E. L. Amma, *Inorg. Chem., 5,* 1966, 1775.
[7] R. W. Baker, M. J. Braithwaite, R. S. Nyholm, *J. Chem. Soc. Dalton Trans.*, 1972, 1924.
[8] R. Favez, R. Roulet, A. A. Pinkerton, D. Schwartzenbach, *Inorg. Chem., 19,* 1980, 1356.
[9] Th. A. van der Knapp, Th. C. Klebach, F. Visser, F. Bickelhaupt, P. Ros, E. J. Baerends, C. H. Stam, M. Konijn, *Tetrahedron, 40,* 1984, 765.
[10] M. J. Hopkinson, H. W. Kroto, J. F. Nixon, N. P. C. Simmons, *J. Chem. Soc. Chem. Commun.*, 1976, 513.
[11] H. W. Kroto, J. F. Nixon, K. Ohno, *J. Mol. Spectrosc., 90,* 1981, 367.
[12] H. W. Kroto, J. F. Nixon, O. Ohashi, K. Ohno, N. P. C. Simmons, *J. Mol. Spectrosc., 103,* 1984, 113.
[13] A. Appel, C. Casser, M. Immenkeppel, F. Knoch, *Angew. Chem. Int. Ed. Engl., 23,* 1984, 895.
[14] D. Gudat, E. Niecke, A. M. Arif, A. H. Cowley, S. Quashie, *Organometallics, 5,* 1986, 593.
[15] S. S. Al-Juaid, P. B. Hitchcock, R. M. Matos, J. F. Nixon, *J. Chem. Soc. Chem. Commun.*, 1993, 267.
[16] R. Bartsch, P. B. Hitchcock, J. F. Nixon, *J. Chem. Soc. Chem. Commun.*, 1989, 1046.
[17] G. Becker, W. Hölderich, *Chem. Ber., 108,* 1975, 2484.
[18] G. Becker, *Z. Anorg. Allg. Chem., 430,* 1977, 66.
[19] R. Bartsch, J. F. Nixon, unpublished results.
[20] G. Becker, W. Becker, R. Knebl, H. Schmidt, U. Weeber, M. Westerhausen, *Nova Acta Leopold., 59,* 1985, 55.